JOURNAL OF SOLID STATE CHEMISTRY **80**, 68–74 (1989)

An X-Ray Powder Diffraction Study of the $NdBr_3$–$TbCl_3$ System

M. OLEJAK-CHODAN AND H. A. EICK*

Department of Chemistry, Michigan State University,
East Lansing, Michigan 48824-1322

Received October 25, 1988; in revised form February 6, 1989

The $NdBr_3$–$TbCl_3$ system has been investigated by the Guinier X-ray powder diffraction technique over the full composition range. Four discrete phase regions were identified. Orthorhombic $PuBr_3$-type solid solution regions were observed from 0 to ~12.5 and 52.5 to 100 mole% $NdBr_3$. A hexagonal UCl_3-type region was apparent between 5 and ~60 mole% $NdBr_3$, and a monoclinic $AlCl_3$-type region was found between ~15 and 50 mole% $NdBr_3$. Between 7.5 and ~17.5 mole% $NdBr_3$ a high-temperature phase which could not be characterized was also observed. Phase limits in the 7.5–17.5 mole% region were particularly sensitive to annealing conditions.

Introduction

Studies of mixed trihalide systems LnX_3–$Ln'Y_3$, where Ln and Ln' represent different lanthanoid elements and X and Y are the Cl, Br, or I anions, provide unique opportunities to examine the effects of slight cation and anion size differences on structural properties. Numerous lanthanoid mixed-halide ternary systems have recently been examined by X-ray diffraction and thermal techniques (*1–3*). Exemplary systems (with the structure types indicated in parentheses) are: $LaCl_3$–$LaBr_3$ (UCl_3–UCl_3), $NdCl_3$–$NdBr_3$ (UCl_3–$PuBr_3$), $GdCl_3$–$DyCl_3$ (UCl_3–$AlCl_3$), $TbCl_3$–$TbBr_3$ ($PuBr_3$–$AlCl_3$), $DyCl_3$–$HoCl_3$ ($AlCl_3$–$AlCl_3$), and $YbCl_3$–$YbBr_3$ ($AlCl_3$–$FeCl_3$). Nonisomorphous parent phases usually produce either eutectic structures or two solid solution regions with one or more different structure-type phase also present between these solid solution regions (*2–4*). Isomorphous systems, on the other hand, typically exhibit only continuous solid solution over the full composition range (*1, 2, 4*). Isomorphous solid solution behavior has been observed with different-sized cations in the $DyCl_3$–$HoCl_3$ system (*2*) and with different-sized anions in the $LaCl_3$–$LaBr_3$ system (*1*).

The quaternary $TbCl_3$–$NdBr_3$ system in which both parent phases exhibit the $PuBr_3$-type structure is of particular interest. In the $TbCl_3$–$TbBr_3$ system with increasing mole% $TbBr_3$ a $PuBr_3$-type solid solution region, a two-phase region, and an extended $AlCl_3$-type solid solution region are found (*3*). In the $NdCl_3$–$NdBr_3$ system with increasing mole% $NdBr_3$ an extended UCl_3-type solid solution region, a two-phase region, and a narrow $PuBr_3$-type solid solution region prevail (*1*).

The CN VIII ionic radii of Tb^{3+} and Nd^{3+} differ by 0.07 Å; the CN VI radii of Cl^- and Br^- differ by 0.15 Å (*5*). However, the volume mismatch, defined as $(V_2-V_1)/V_{12}$,

---

* To whom correspondence should be addressed.

0022-4596/89 $3.00

where V_{12} represents the mean of the two molar volumes, is 0.209 (*4*). Thus, even though on the basis of parent structure types this $NdBr_3$–$TbCl_3$ system might exhibit continuous solid solution (*4*), both the limited solubility of bromide ions in $TbCl_3$ and chloride ions in $NdBr_3$ (*1, 3*) and potential changes in the structure caused by the internal pressure which results from the presence of different-sized ions (*6*) were expected to make the phase relationships complex and unpredictable. Consequently, a systematic study of the title system was undertaken; its results are presented below.

Experimental

The reactants $TbCl_3$ and $NdBr_3$ were synthesized, respectively, from Tb_2O_3 (prepared by hydrogen reduction of "Tb_4O_7") and Nd_2O_3 (both 99.9%, from Michigan Chemical Co.). Synthesis was effected according to the ammonium halide matrix procedure (*7, 8*) with NH_4Cl (ACS reagent grade, Fisher Scientific) in a 1 : 6 molar ratio and NH_4Br (ACS reagent grade, Matheson) in a 1 : 8 molar ratio as described previously (*3*). The trihalides were purified by distillation at 10^{-6} Torr (*9*). All manipulations of reactants and products were effected in a glove box whose Ar atmosphere was continuously purged of H_2O (molecular sieves) and oxygen (heated BASF catalyst).

The $TbCl_3$–$NdBr_3$ system was studied over the full composition range in steps of 2.5, 5, or 10 mole% depending upon the nature of the results. Mixed trihalide specimens, each of which had a total mass of 0.3 g, were intimately ground in an agate mortar in the desired stoichiometric ratio according to:

$$xTbCl_3 + (1 - x)NdBr_3 \rightarrow Tb_xNd_{(1-x)}Cl_{3x}Br_{(3-3x)}. \quad (1)$$

After transfer to 7-mm-i.d. previously outgassed quartz tubes the samples were melted with a hand torch under a vacuum of 10^{-3} Torr and then quenched to room temperature. Selected specimens (7.5, 10, 17.5, 20, and 52.5 mole% $NdBr_3$) were resealed into outgassed quartz tubes, heated in a Thermco Minibrute furnace to 588°C, the $TbCl_3$ melting point (*9*), cooled at 2°C/hr to 400°C, then left to cool in the oven which was shut off. Two other resealed specimens (10 and 12 mole% $NdBr_3$) were heated to 580°C, cooled at 5°C/hr to 320°C, and then at 30°C/hr to room temperature. All products were pulverized in an agate mortar and examined in an evacuated 114.6-mm-diameter Guinier–Hägg X-ray camera with Cu$K\alpha_1$ ($\lambda\alpha_1$ = 1.54050 Å) radiation and NBS certified Si (a = 5.430825(36) Å) as internal standard. Reflection positions were determined as described previously (*3*). Lattice parameters were determined initially with a locally written least-squares program and refined subsequently with the program APPLEMAN (*10*). For selected compositions theoretical X-ray powder reflection intensities were calculated with the program POWD12 (*11*); calculations were effected on a VAX 11/750.

Results

Mass balance confirmed that the final composition could be considered identical to the mixed composition. There was no apparent attack of the quartz container during the short interval that the samples were molten. Even specimens that were annealed over a period of 4 days did not attack the quartz container appreciably. Oxidehalide reflections were never observed.

Both $TbCl_3$ and $NdBr_3$ reagents crystallized in the $PuBr_3$-type (*Cmcm*) structure (*12*). The observed lattice parameters for these reagents are in good agreement with literature values (*13, 14*); observed intensities corresponded well to calculated values. Lattice parameters for these parent phases and for the phases present at selected com-

TABLE I

LATTICE PARAMETER DATA FOR SELECTED COMPOSITIONS IN THE $NdBr_3$–$TbCl_3$ SYSTEM

Overall composition	% $TbCl_3$	Struct. type	a (Å)	b (Å)	c (Å)	β (°)	Ref.[a]
$TbCl_3$	100	$PuBr_3$	3.847(2)	11.771(5)	8.516(4)		(*12*)
			3.846(1)	11.766(5)	8.515(3)		
$Tb_{0.95}Nd_{0.05}Cl_{2.85}Br_{0.15}$	95	$PuBr_3$	3.857(2)	11.845(5)	8.546(2)		
$0.9(TbCl_3) \cdot 0.1(NdBr_3)$	90	UCl_3[b]	7.403(1)		4.112(1)		
		UCl_3[c]	7.410(4)		4.132(6)		
		$PuBr_3$[c]	3.85(1)	11.86(2)	8.58(1)		
$0.8(TbCl_3) \cdot 0.2(NdBr_3)$	80	UCl_3	7.448(1)		4.158(2)		
		$AlCl_3$	7.031(2)	12.177(1)	6.58(1)	110.74(1)	
$0.7(TbCl_3) \cdot 0.3(NdBr_3)$	70	UCl_3	7.503(9)		4.194(1)		
		$AlCl_3$	7.048(5)	12.209(7)	6.577(1)	110.93(1)	
$0.6(TbCl_3) \cdot 0.4(NdBr_3)$	60	UCl_3	7.562(2)		4.221(4)		
		$AlCl_3$	7.095(4)	12.282(5)	6.633(4)	110.69(1)	
$0.5(TbCl_3) \cdot 0.5(NdBr_3)$	50	UCl_3	7.623(2)		4.259(3)		
		$AlCl_3$	7.124(3)	12.343(4)	6.687(3)	110.96(1)	
$0.47(TbCl_3) \cdot 0.53(NdBr_3)$	47	UCl_3	7.637(1)		4.264(1)		
$Tb_{0.35}Nd_{0.65}Cl_{1.05}Br_{1.95}$	35	$PuBr_3$	4.040(1)	12.501(4)	9.001(2)		
$NdBr_3$	0	$PuBr_3$	4.108(6)	12.637(9)	9.141(7)		
			4.10(3)	12.63(5)	9.15(4)		(*13*)

[a] This work, except as noted.
[b] Quenched.
[c] Annealed.

positions are presented in Table I. Phase relationships in the mixed-halide system are presented schematically in Fig. 1. In this system orthorhombic $PuBr_3$-type solid solution regions extend from 0 to ~12.5 and from 52.5 to 100 mole% $NdBr_3$. A hexagonal UCl_3-type region is found between 5 and ~60 mole% $NdBr_3$, and a monoclinic $AlCl_3$-type region spans ~15 to 50 mole% $NdBr_3$. Between 7.5 and ~17.5 mole% $NdBr_3$ two

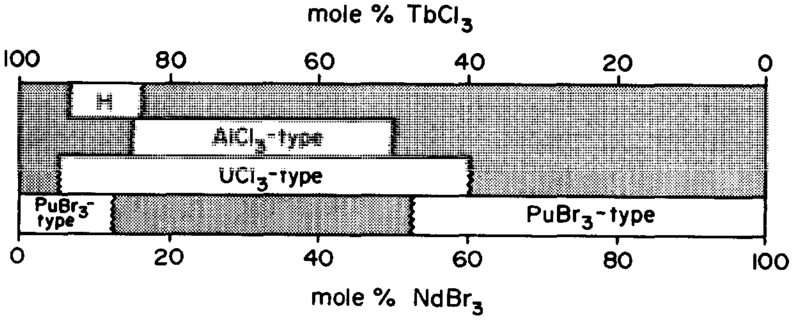

FIG. 1. A schematic representation of the $TbCl_3$–$NdBr_3$ system as a function of composition. The blocks represent the composition range over which the designated phase is observed in the X-ray diffraction pattern. The letter *H* represents a quenchable high-temperature modification. Diphasic regions span 5–~12.5, ~15–50, and 52.5–~60 mole% $NdBr_3$.

interplanar composition dependent *d*-spacings (with intensities), 5.464 (vvw) and 4.667 Å (m), which could not be assigned to any expected phase were observed consistently along with the $PuBr_3$- and UCl_3-type reflections in the quenched specimens. The annealed 7.5, 10, and 12.5 mole% $NdBr_3$ specimens, on the other hand, did not evidence these reflections.

The various diphasic regions, expressed in terms of mole% $NdBr_3$, and the structure types observed in them are: 5 to ~12.5, $PuBr_3$- and UCl_3-types; ~15 to 50, UCl_3- and $AlCl_3$-types; and 52.5 to ~60, UCl_3- and $PuBr_3$-types. Monophasic regions, expressed in terms of mole% $NdBr_3$, span 0 to 5, $PuBr_3$-type; ~12.5 to 15 and 50 to 52.5, UCl_3-type; and 60 to 100, $PuBr_3$-type.

Discussion

Assignment of X-ray reflections to the $PuBr_3$- and UCl_3-type structures was straightforward. The UCl_3-type reflections corresponded very closely to those in the UCl_3-type region of the Gd–Cl–Br system, and assignment could be made visually by comparing adjacently situated Guinier diffraction films. Assignment of the remaining reflections to the $AlCl_3$-type structure, on the other hand, was tenuous and difficult. In both the Gd–Cl–Br and Tb–Cl–Br systems this monoclinic structure was characterized by broad, weak reflections. After UCl_3-type reflections had been assigned in this quaternary system, typically only eight broad frequently weak reflections remained, and these in addition to potential superpositions based upon intensity considerations constituted the evidence for the monoclinic phase. However, the accuracy of this assignment is enhanced by X-ray powder intensity calculations which indicate that for the $AlCl_3$ phase the first reflection should be the most intense (*11*). It should be followed first by weaker reflections, and then by very weak reflections. This pattern of intensity variation was observed for the 15–50 mole% $NdBr_3$ specimens.

The two extra X-ray reflections apparent in the 7.5–~17.5 mole% $NdBr_3$ region could not be assigned definitively to the $FeCl_3$- or the high-pressuure RhF_3- or $PuBr_3$-type structures common to species with these radius ratios (*15–17*). Nor could they be assigned to oxide or oxidehalide phases or to known hydrate phases. (Hydrate phases were not expected since the moisture level in the glove box was typically 3.5 ppm_v, as recorded on an ONDYNE moisture content monitor when experiments were being repeated.) The inability to assign these two reflections to any known phase, their variation with composition, and the fact that annealed specimens do not exhibit them suggest strongly that they result from a quenched high-temperature modification. The phase can only be characterized by increasing its concentration, probably through either high-temperature X-ray or high-pressure experiments, or through more rapid quenching.

The region 7.5–17.5 mole% $NdBr_3$ was difficult to interpret as the results depend upon annealing conditions. For example, in the 5°C/hr annealed 10 mole% specimen the moderately intense 5.464 and 4.667 Å reflections were absent, but three very weak (7.785, 7.181, 3.952 Å) and one weak (3.1696 Å) reflection in addition to clearly indexable UCl_3- and $PuBr_3$-type reflections were present. The quenched 10 and 12 mole% specimens did not evidence any $PuBr_3$-type reflections, whereas these reflections were relatively intense in the same specimens when they were annealed. On the other hand, annealing did not appear to affect other regions of the system as dramatically. The diagram presented in Fig. 1 is based upon results obtained from annealed specimens.

Solid solution regions prevail at both ends of the system. The solubility of $NdBr_3$

in $TbCl_3$ is modest compared to that of $TbCl_3$ in $NdBr_3$. The former exhibits only a ~12.5 mole% solubility range; the latter exhibits a 47.5 mole% solubility range. The low solubility of $NdBr_3$ in $TbCl_3$ is reminiscent of that observed in the $NdCl_3$–$NdBr_3$ ternary system (*1*) in which a $PuBr_3$-type structure prevailed only over a ~5 mole% range; the UCl_3-type structure which is common to $NdCl_3$ then appeared. The appearance of the UCl_3-type structure in this work at a relatively low mole percentage substitution limit provides insight into the atomic distribution as is discussed below.

For the most part the system behavior can be interpreted from radius ratio considerations, where radius ratio is defined as $R = r(X^-)/r(M^{3+})$, even though quantitative radius ratio calculations are not meaningful for mixed systems such as these. In both the $LnCl_3$ and $LnBr_3$ systems one observes the following structure types with increasing R: UCl_3-, $PuBr_3$- (which for $LnCl_3$ prevails over a relatively narrow R region), $AlCl_3$- (which for $LnBr_3$ is stable over a very narrow R region), and finally the $FeCl_3$-type structure (*3, 15*). R for $NdBr_3$ and $TbCl_3$ are reported in (*18*) as 1.960 and 1.961, respectively; they are 1.45 and 1.41, respectively, based on Shannon's radii (*5*).

In this system as $NdBr_3$ is added to pure $TbCl_3$ the Nd^{3+} and Br^- ions substitute into the $TbCl_3$ lattice and the radius ratio as it pertains to any particular cation can effectively either be increased or decreased, depending upon the distribution of anions around that cation. If solid solution with a random atomic distribution continued to prevail, the $PuBr_3$-type structure should persist. However, the UCl_3-type structure appears. This unexpected appearance is indicative of some level of cation and anion ordering, or preference, i.e., Cl^- anions must preferentially coordinate Nd^{3+} cations and Br^- anions must preferentially coordinate Tb^{3+} cations, as is discussed later.

The opposite (high $NdBr_3$ mole%) end of the system exhibits an extended $PuBr_3$-type solubility region that bears little resemblance to the behavior observed in the ternary Tb–Cl–Br system (*3*), apparently because extensive cation substitution (Nd^{3+} for Tb^{3+}) has occurred and changed the effective Ln^{3+} radius. In the ternary Tb–Cl–Br system the $PuBr_3$-type structure prevailed only to the ~15 mole% tribromide composition while in the ternary Gd–Cl–Br system this structure prevailed over a 25 mole% range, from 20 to 45 mole% tribromide. The present behavior is reflective of the $PuBr_3$-type solubility regions exhibited by *both* of these systems. With an effective cation radius larger than that of Tb^{3+} (because of the presence of Nd^{3+}) which increases as the $NdBr_3$ content is increased, the R range over which the $PuBr_3$-type structure retains stability appears extended and approximates that of *both* the Tb–Cl–Br and Gd–Cl–Br systems. Again, as $TbCl_3$ is added to $NdBr_3$ and by analogy to the Gd–Cl–Br ternary system (*3*), Cl^- anions selectively coordinate the larger Nd^{3+} and favor UCl_3-type structure formation. It is consequently the first phase that appears near the end of the $NdBr_3$ extended solid solution region (from 52.5 to 100 mole% $NdBr_3$, or from 0 to 47.5 mole% $TbCl_3$). Ion segregation of Cl^- anions in the UCl_3-type phase causes an $AlCl_3$-type phase to appear soon thereafter with concomitant disappearance of the $PuBr_3$-type structure.

It is helpful to think of the entire system in terms of changing R values. If one imagines starting with pure $TbCl_3$ and substituting Nd^{3+} for Tb^{3+} and Br^- for Cl^- only the common $PuBr_3$-type structure persists to the solubility limit discussed previously, ~5 mole%. Beyond this solubility limit a significant cation and anion reordering occurs. The appearance of the UCl_3-type $Nd(Cl,Br)_3$ phase (found with small R values) indicates that the Cl^- ions have combined predominantly with the Nd^{3+} cations, and the Br^- anions with the Tb^{3+} cations. The molar volume of the UCl_3-type structure at the 10 mole% $NdBr_3$ composition, the minimum composition for which parameters could be determined, is 195.2 Å^3, and is very close to that of pure $NdCl_3$ (200.4 Å^3). This UCl_3-type phase persists to the 60 mole% $NdBr_3$ composition; in the ternary Nd–Cl–Br system the UCl_3-type structure prevails to 70 mole% tribromide. This small difference is presumed to result because the limited cation miscibility has effectively altered slightly the cation radius.

At ~12.5 mole% $NdBr_3$, as a result of Cl^- ions combining preferentially with Nd^{3+} cations in the UCl_3-type phase, the effective size of those anions associated with Tb^{3+} has increased such that the $PuBr_3$-type structure can no longer be sustained. The structure type common for larger R values, the $AlCl_3$-type structure, which spans the range $\sim 1.993 < R < \sim 2.079$ (*18*), and the UCl_3-type region, which spans the radius ratio range $\sim 1.706 < R < \sim 1.930$ (*18*), then prevail. As the $NdBr_3$ content is increased, the ions are distributed preferentially between the UCl_3- and $AlCl_3$-type phases, and the radius ratio values associated with each of these phases slowly converge. At 50 mole% $NdBr_3$ the $AlCl_3$-type phase disappears and at 52.5 mole% $NdBr_3$ local R values are such that the $PuBr_3$-type phase reappears. The UCl_3-type (predominantly) $Nd(Cl,Br)_3$ material by now has become adequately Br^--rich so that it too converts to the $PuBr_3$-type structure; this structure type prevails thereafter.

Although the behavior of this mixed system and the phases observed can be understood on the basis of radius ratio considerations, the presence of the UCl_3-type structure which exists over an effective radius ratio range *smaller* than that of either pure phase was not expected. Only a nonrandom cation/anion arrangement could create effective radii that would allow this structure-type field of stability to persist over such an extended range. The nine-coordinate UCl_3-type structure is exhibited by $LnCl_3$ species for Ln = La–Gd. Thus Nd is near the middle of this field of stability. Presumably the greater stabilization which results from the higher coordination provided by Cl^- anions supplies the driving force that selectively concentrates Cl^- anions in this phase. On the other hand, $TbBr_3$ is near the interface of the six-coordinate–eight-coordinate stability region. The Tb^{3+} ion by combining preferentially with Br^- anions not only achieves more optimum coordination stability, but also contributes to the driving force needed to separate the anions.

Observation of a quenchable high-temperature modification that disappeared upon annealing and the differing phase limits observed in the 7.5–17.5 mole% $NdBr_3$ region with annealing demonstrate the phase limit dependence upon thermal treatment. Under different thermal conditions slightly different phase limits might be observed.

Acknowledgment

Support of the National Science Foundation, Division of Materials Research, Solid State Chemistry Program, DMR 84-00739, is acknowledged gratefully.

References

1. M. Olejak-Chodan, S. A. Hodorowicz, and H. A. Eick, *Lanthanide Actinide Res.* **2,** 3–8 (1987).
2. G. Garton and P. J. Walker, *Mater. Res. Bull.* **17,** 1227–1234 (1982).
3. M. Olejak-Chodan, W. Lasocha, and H. A. Eick, *J. Solid State Chem.* **73,** 259–267 (1988).
4. P. K. Davies and A. Navrotsky, *J. Solid State Chem.* **46,** 1–22 (1983).
5. R. D. Shannon, *Acta Crystallogr. Sect. A* **32,** 751–767 (1976).
6. E. K. Hodorowicz, S. A. Hodorowicz, and H. A. Eick, *J. Solid State Chem.* **52,** 156–162 (1984).
7. M. D. Taylor, *Chem. Rev.* **62,** 503–511 (1962).
8. G. Meyer and P. Ax, *Mater. Res. Bull.* **17,** 1447–1455 (1982).

9. D. E. Cox and F. K. Fong, *J. Cryst. Growth.* **20,** 233–238 (1973).
10. D. E. Appleman, D. S. Handwerker, and H. T. Evans, "Program X-Ray," Geological Survey. U.S. Dept. of Interior, Washington, DC (1966).
11. D. K. Smith, M. C. Nichols, and M. E. Zolensky, "A FORTRAN IV Program for Calculating X-Ray Powder Diffraction Patterns: Version 10." Pennsylvania State University, University Park (1983).
12. J. M. Haschke, *J. Solid State Chem.* **18,** 205–216 (1976).
13. A. Murasik, P. Fischer, A. Furrer, and W. Szczepaniak, *J. Less-Common Met.* **111,** 177–184 (1985).
14. W. H. Zachariasen, *Acta Crystallogr.* **1,** 265–268 (1948).
15. H. P. Beck and E. Gladrow, *Z. Anorg. Allg. Chem.* **453,** 79–82 (1979).
16. H. P. Beck and E. Gladrow, *Z. Anorg. Allg. Chem.* **498,** 75–84 (1983).
17. H. P. Beck and E. Gladrow, *Z. Anorg. Allg. Chem.* **502,** 178–184 (1983).
18. D. Brown, S. Fletcher, and D. G. Holah, *J. Chem. Soc. A* **1968,** 1889–1894 (1968).